Journal of Polymer Research (2021) 28: 410
https://doi.org/10.1007/s10965-021-02761-1

ORIGINAL PAPER

Development of polyvinyl (alcohol)/D-glucose/agar/silver nanoparticles nanocomposite film as potential food packaging material

Bao-Tran Tran Pham[1] · Thuy-Hang Thi Duong[2] · Thuong Thi Nguyen[1,3,4] · Dai Van Nguyen[5] · Chinh Dung Trinh[6] · Long Giang Bach[1]

Received: 3 April 2021 / Accepted: 16 September 2021 / Published online: 6 October 2021

Abstract

The functional nanocomposite films from polyvinyl (alcohol) (PVA), D-glucose, agar, and silver nanoparticles (AgNPs) components were synthesized through the facile casting method. Results from the evaluation of antimicrobial activity and composite film properties showed that the combination of PVA/D-glucose/agar with AgNPs significantly enhanced bactericidal activity against *Escherichia coli, Pseudomonas aeruginosa*, and *Staphylococcus aureus*, as well as mechanical property. Furthermore, the coating from the combination of PVA/D-glucose/agar with AgNPs was also applied in Areca banana preservation for 7 days at 25 ℃. Appearance, physiological weight loss, total soluble sugars, and titratable acidity were daily evaluated during storage period. The obtained results of this study show the promising potential of PVA/D-glucose/agar nanocomposite film incorporated with AgNPs for food packaging applications in the near future.

Keywords Polyvinyl (alcohol) · Silver nanoparticles · Mechanical properties · Antimicrobial · Food packaging film

Introduction

Petroleum-based packaging materials existing in the environment is going to seriously effect on soil and water, altering the physical properties of soil, causing soil erosion, preventing soil unable to retain water and nutrients and oxygen from passing through the soil which is harmful to plant growth, and even indirectly affect to human health [1]. To address the aforementioned problems, biodegradable materials have become favorite in food packaging area, especially polymers derived from natural sources, such as chitosan [2–5], nanocellulose [6, 7], starch [8–10], gelatin [11, 12] in food packaging area, were investigated. Although polyvinyl (alcohol) (PVA) is a synthesis polymer, it is widely used as a food packaging material by virtue of its biocompatibility, biodegradability, cost-efficiency [13]. However, PVA is unlimitedly soluble in water owing to the high density of hydroxyl group along backbone which has a strong affinity with water molecules, limiting its application in food packaging field, because of the high hydrophilic property on film surface facilitates bacterial growth [14, 15]. To reduce the hydrophilicity of PVA, various chemical and physical methods have been performed for the purpose of cross-linking PVA [16–20]. Agar, a polysaccharide with a linear structure, composes of β-D-galactopyranose and 3,6-anhydro-α-L-galactopyranose repeating units linked together by β-1,4 and α-1,3 glycosidic linkages [21]. As expected, many –OH groups in agar's structure, possibly interact with –OH groups in PVA chains resulting in limiting infinite solubility in water of PVA. Therefore, agar is considered to be an excellent candidate for the improvement of the hydrophobicity of

✉ Thuong Thi Nguyen
nthithuong@ntt.edu.vn

1 Institute of Environmental Sciences, Nguyen Tat Thanh University, Ho Chi Minh City, Vietnam

2 Faculty of Chemical Technology, Ho Chi Minh City University of Food Industry, Ho Chi Minh City 705800, Vietnam

3 Faculty of Chemistry, University of Science, Ho Chi Minh City 72711, Vietnam

4 Vietnam National University, Ho Chi Minh City 700000, Vietnam

5 Faculty of Automobile Technology, Van Lang University, Ho Chi Minh City, Vietnam

6 Institute for Nanotechnology, Ho Chi Minh City 700000, Vietnam

PVA films [22]. However, PVA/agar film has high moisture [22], which may attract the growth of microorganisms and hence they do not meet the basic properties of food packaging film. D-glucose, the constituent of polysaccharide and good film-forming agent, is used to reduce recrystallization, improve stability, and reduce hydrophilicity of film during food storage period [23]. In the previous study, we have successfully modified PVA with D-glucose and agar with the aim of improving their hydrophobicity and thermal stability of PVA [24].

Active food packaging based on PVA was generated through the incorporation of antimicrobial agent [25–28]. Herein, silver nanoparticles (AgNPs), are extensively used in packaging films for the purpose of enhancing antimicrobial activity of food preservation [6, 29–31], due to their unique properties such as their antibacterial ability to against *Staphylococcus*, *Enterococcus*, *Pseudomonas*, and *Enterobacteriaceae* [6, 30, 32]. The plethora of reports exhibited positive effect of incorporated AgNPs on the properties of resultant films. For instance, the AgNPs combination with PVA/nanocellulose film reported by Sarwar et al. [6] improved tensile strength of the resulting film more than twice. Meanwhile, the addition of AgNPs offered the increase in antimicrobial activity of PVA [6, 33, 34], agar [35, 36], chitosan [35–37] films.

In present study, we aim to develop food packaging films by combining PVA modified with D-glucose, agar, and AgNPs for the first time. Film properties characterized by scanning electron microscope (SEM), energy dispersive spectroscopy (EDS Mapping), UV–Vis, the attenuated total reflectance Fourier transform infrared (ATR-FTIR), X-ray diffraction (XRD), color values, mechanical properties, solubility, and antibacterial properties of the films were investigated in detail. The coating from PVA/D-glucose/agar and AgNPs was also applied to preserve Areca banana at 25 ℃ for 7 days. The banana's appearance and nutrition during storage period were also assessed.

Materials and methods

Materials

Polyvinyl (alcohol) (PVA) cold water soluble with M_w ~ 160,000 g/mol and 10–12% of acetate content, D-glucose ($C_6H_{12}O_6$, 99% purity), and silver nanoparticles were purchased from HiMedia (HiMedia Laboratories Pvt., Ltd, India). Agarose powder ($(C_6H_{10}O_5)_n$, was provided by VWR (Van Water & Rogers part of Avantor, France). All other reagents, including Sodium hydroxide (NaOH) (98%) and phenolphthalein were of analytical grade without further purification.

Film preparation

Preliminary tests on the nanocomposite films to choose appropriate amount of AgNPs loaded into polymer blend of PVA, D-glucose, and agar (Supplementary Fig. S1). All PVA-based films were prepared via casting method as well-described in Scheme 1. The solution of D-glucose (1%, wt/v) and agar (1%, wt/v) was mixed with PVA solution (3%, wt/v) and stirred at 50 ℃ for 1 h. After that, 30% (wt/wt) of glycerol (in comparison to the total weight of solids) was added into the mixture solution as a plasticizer. The solution was

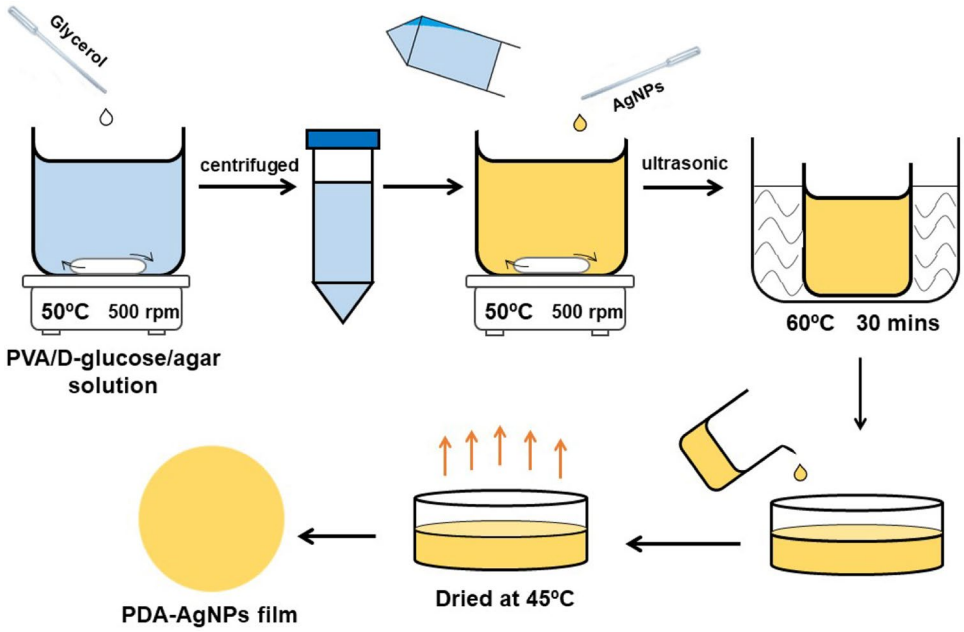

Scheme 1 PVA/D-glucose/agar incoporated with AgNPs film forming process

then stirred at 50 ℃ for 1 h to get a miscibility solution, remarked as PDA. The PDA solution was further centrifuged to remove bubbles and impurities. Subsequently, three different AgNPs concentrations of 0.185 mM, 0.370 mM, and 0.555 mM were added into the centrifuged PDA solution and further sonicated for 30 min at 60 ℃ and labeled PDA-AgNPs-0.185, PDA-AgNPs-0.370, and PDA-AgNPs-0.555, respectively (Supplementary Table S1). Finally, the PDA and PDA-AgNPs solutions were cast on the plastic molds and then dried at 45 ℃ for 60 h. The dried films were peeled off and stabilized at 25 ℃ for 24 h before analyses.

Characterization of films

The surfaces of PDA-AgNPs films were observed by scanning electron microscope (SEM) and EDS Mapping. SEM was conducted on Hitachi S-4800 (JEOL Ltd., Japan) at a magnification of 7500 and voltage of 5 kV. EDS Mapping was determined on Oxford Instrument NanoAnalysis (Oxford Instruments Inc., France).

The color properties of films were measured by using the Konica Minolta Chroma Meter Model CR-400 (Konica Minolta Inc., Japan). Color of the films was expressed as L (brightness/lightness), a (greenness/redness), and b (blueness/yellowness) values. The aforementioned parameters were measured by placing film pieces (20 mm in diameter) on a standard white plate (L* = 93.57, a* = –0.24, and b* = 3.6) Total color differences (ΔE) and whiteness index (WI) was calculated by the following equation [38]:

$$\triangle E = \sqrt{\left(L^* - L\right)^2 - (a^* - a)^2 - \left(b^* - b\right)^2} \quad (1)$$

$$WI = 100 - [(100 - L)^2 + a^2 + b^2]^{\frac{1}{2}} \quad (2)$$

where L*, a*, and b* are the color parameter values of the standard and L, a, and b are the color parameter values of the films.

The thickness of films was measured by using a digital micrometer (Mitutoyo Co., Japan).

The UV–Vis transmittance of films in a wavelength range of 300–800 nm was recorded in a UV-1800 UV/Visible Scanning Spectrophotometer (Shimadzu Co., Japan).

The Attenuated total reflectance Fourier transform infrared (ATR-FTIR) spectra of films were determined by using FT/IR-6600typeA spectrometer equipped with ATR PRO ONE (Jasco International Co., Ltd., Japan).

The X-ray diffraction (XRD) patterns were executed on a D2 PHASER—X-ray diffraction equipment (Bruker Japan K.K., Japan), using Cu-K as radiation source with a velocity of 0.5/s in diffraction angles (2θ) of 5–80°.

Mechanical properties of nanocomposite films including tensile strength, percentage of elongation at break, and elastic modulus were measured in accordance with ASTM D882-02 standard on Universal Testing Machine (Yang Yi Technology Co., Taiwan) with a load cell of 0.5 kN. Eight specimens of each film (15 mm wide and 120 mm long) were tested under the crosshead speed of 50 mm/min at 25 ℃.

Determination of contact angle and solubility

The hydrophobic/hydrophilic nature of PVA-based films was determined through contact angle measurement on Theta Optical Goniometer (KSV Instruments Co., USA). Solubility was determined following the method described by Souza et al. with some modifications [39]. The films were cut into a rectangle (25 × 25 mm) and weighted using an analytical balance with a precision of 0.1 mg to get initial weight then dried at 50 ℃ specimens for 24 h to get the initial dry mass (M_1). After that, films were immersed in 30 mL distilled water at room temperature (25 ℃) and taken off after 24 h. The residual water on the surface of the films was dried by tissue paper and the specimens after water absorption were further weighed. Then, the films were dried at 50 ℃ for 24 h to determine the final dry mass (M_2). The experiments were replicated at least 3 times for each film to calculate average values via the following equation:

$$\text{Solubility } (\%) = \frac{(M_1 - M_2)}{M_1} \times 100 \quad (3)$$

Antibacterial test

The antimicrobial activity of PDA films with and without AgNPs was conducted through the disc diffusion method reported by Tepe et al. [40] with a minor change. *Pseudomonas aeruginosa* NRRL B-14781 and *Escherichia coli* NRRL B-409 were chosen as Gram-negative (-) bacterial models and *Staphylococcus aureus* NRRL B-313 was chosen as Gram-positive (+) bacterial models. Bacterial strains were incubated 24 h at 37 ℃ in Luria–Bertani agar. Firstly, suspension of the tested microorganism (100 µL of 2 × 10^6 CFU/mL) was poured and diffused on the solid media plates. Then, square films (1 × 1 cm) were placed on the plate containing bacteria and further incubated at 37 ℃ for 24 h. The inhibition zone diameter of the films was measured in millimeter unit. All tests were replicated three times for each composition.

Application of PDA-AgNPs coating for Areca banana preservation

Areca bananas were selected for uniformity of weight and maturity. The bananas were further washed with distilled

water and dried naturally at room temperature (25 ℃). The bananas were divided into 3 random lots including uncoated fruits, fruits coated with PDA and PDA-AgNPs-0.185. The coated bananas were dipped in PDA and PDA-AgNPs-0.185 solution for 5 s and the process was repeated three times after a 15-min interval and stored at room temperature (25 ℃). Five bananas were observed and randomly selected to analyze physicochemical characteristics and nutrition evaluation, then the results were compared with uncoated fruits.

The respiration rate of bananas was determined by using the oxygen and carbon dioxide headspace gas analyzer GS6000 (Systech Instrument Ltd and Illinois Instruments Inc., USA).

The different weight loss was measured daily during storage. The weight loss percentage was calculated as follows:

$$\text{Weight loss } (\%) = \frac{\text{Weight of the first day (g)} - \text{Weight after interval (g)}}{\text{Weight of the first day (g)}} \quad (4)$$

The total soluble sugars content (TSS) of the fruits was measured by using a hand refractometer PR-32α (Atago Co., Ltd., Japan) and the results were expressed in %Brix. The pH of the fruit juice was measured by using a multi-parameter analyzer Consort C3050T Bio Electronic Analyzer Kit (Thermo Fisher Scientific Inc., Belgium). Titratable acidity (TA) was determined through titrated method reported by P. Jongsri et al. [41]. The experiment was performed by taking 10 g of banana pulp in 100 mL of distilled water. Then, 10 mL of the banana solution was added 1% phenolphthalein indicator and titrated with NaOH 0.1 N. The TA (%) was determined as follows:

$$\text{TA } (\%) = \frac{V_{NaOH} \times C_{NNaOH} \times 0.067 \times 100}{10(g)} \quad (5)$$

where V_{NaOH} is the volume (mL), C_{NNaOH} is the molarity (N) of NaOH solution and 0.067 is the conversion factor for maleic acid.

Results and discussion

Film morphology, elemental composition, and light transmittance

The surface morphology of PDA before and after the inclusion of AgNPs is observed in Fig. 1. The PDA film exhibits smooth, homogeneous surface, and without bubble or any fracture, demonstrating good compatibility of PVA, agar, and D-glucose components in the film matrix. After combining with AgNPs, the surface of resulting films become rough with slight folds as well as the appearance of different light–dark fields (Fig. 1b–d). It can be likely attributed to the dispersion of AgNPs embedded in the polymer network. Among the AgNPs-loaded films, it can be seen that the film incorporated with 0.370 mM show better distribution of AgNPs on surface of film than others as evidenced by the even size of the dark areas. The surface of the film combined with 0.555 mM AgNPs shows uneven dispersion of AgNPs in the PDA matrix presumably due to some local agglomeration. This may be attributed to the high concentration resulting in poor dispersion of nanoparticles.

In addition, the energy-dispersive X-ray spectroscopy (EDS) was used to confirm the presence of AgNPs on the PDA-AgNPs-0.370 film surface (Fig. 1e). It can be seen that besides the existence of C and O elements, there is also the existence of AgNPs elements, indicating the presence of AgNPs on nanocomposite film surface. This result is in line with SEM analysis.

The UV–Vis is commonly used to determine the presence and shape of metal nanoparticles lying in the reflection of surface plasmon resonance (SPR). UV–Vis spectrum of PDA combined with AgNPs is illustrated in Fig. 2. The films containing AgNPs exhibit the light adsorption peak at 420 nm corresponding to the SPR of AgNPs [42]. This indicates the presence of AgNPs in the polymer matrix. Similarly, the in-situ/ex-situ reduced AgNPs/PVA nanomaterials reported by Ananth et al. [43] showed the characteristic SPR peak of AgNPs was 400 nm (ex-situ) and 429 nm (in-situ). Elshaarawy et al. [44] also reported the present SPR peaks of AgNPs ranged from 406 to 413 nm in poly (imidazolium vanillyl)-grafted chitosan/silver nanocomposites of cotton fabrics. Thus, based on the result from UV–Vis spectrum, the presence of AgNPs in the films is also confirmed which is in accordance with SEM and EDS analysis results. Moreover, the light transmission characteristic of films is of paramount importance in food packaging, determined in visible light region 660 nm [45]. The transparency of PDA at 660 nm is 75.35% presenting high transparency of film; meanwhile, the optical transmittance of nanocomposite film reduced slightly with the combination with AgNPs. Briefly, these results affirmed the successful inclusion of AgNPs into the PVA/D-glucose/agar film.

Visual appearance and film color

Appearance and the see-through properties of food packaging films are key factors as they influence the customer's attraction and decision before buying a product. Visual appearance of the film composed of PVA, D-glucose, and agar is glossy, clear, and smooth (Fig. 3). Upon the incorporation of 0.185–0.555 mM AgNPs, the resulting films are still homogeneous without any wrinkles or bubbles. Meanwhile, the film color turns yellow and the intensity tends to dark red as increasing AgNPs concentration; however, the text still clearly visible, indicating high transparency.

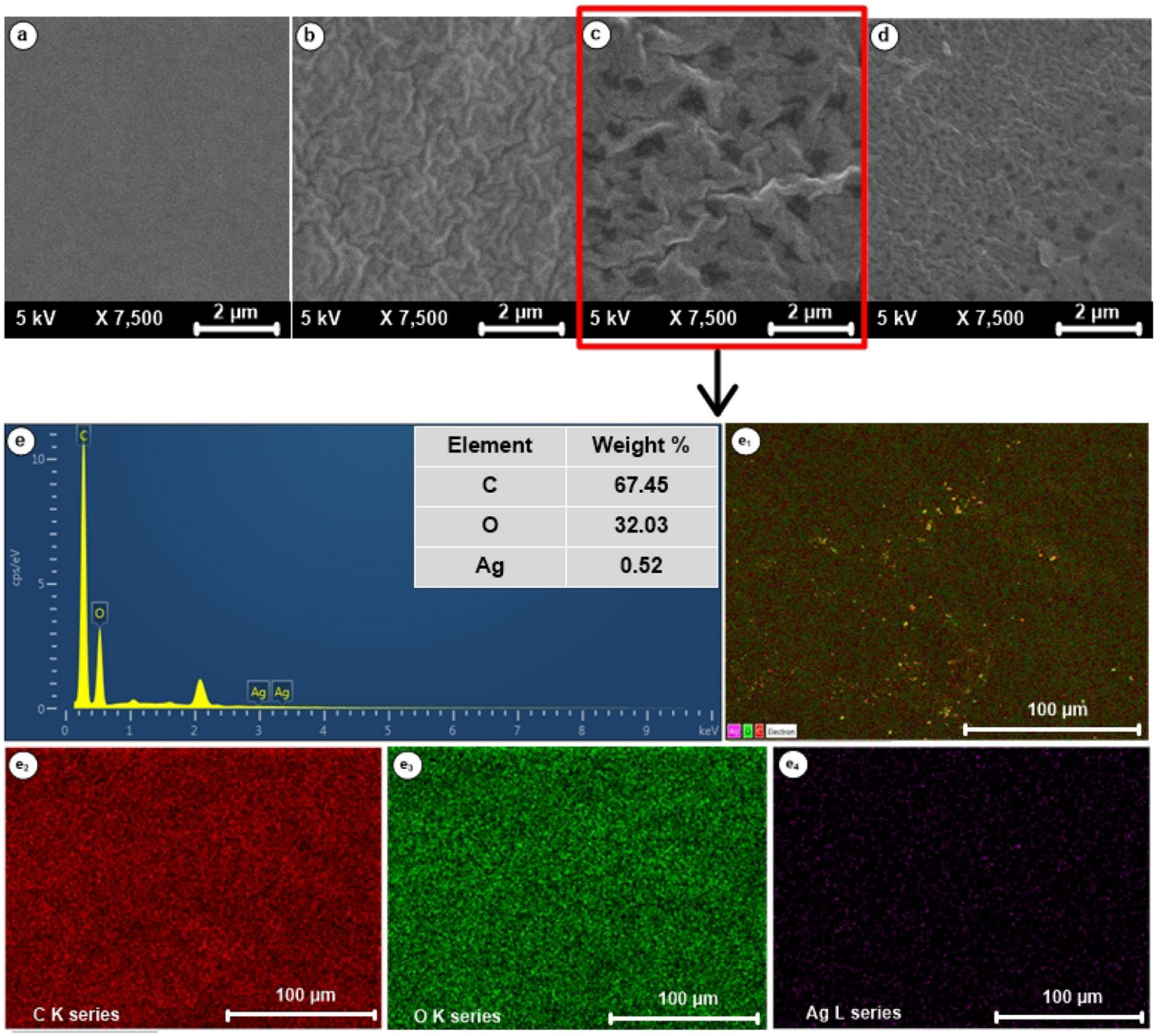

Fig. 1 SEM of PDA (**a**), PDA-AgNPs-0.185 (**b**), PDA-AgNPs-0.370 (**c**), PDA-AgNPs-0.555 (**d**), EDS profile of PDA-AgNPs-0.370 and quantitative analysis (**e**), EDS element mapping data of all displayed elements (e1—e4)

The color of nanocomposite films was also affirmed through color measurement, as shown in Table 1. L, a, and b values of the PDA film is 89.69, -0.31, and 5.20, respectively, implying that PDA film was transparent and colorless as corroborated in visual appearance. After loading AgNPs, some changes in surface color of nanocomposite films are linear with visual appearance. For instance, the L value gradually decreases, with increasing AgNPs content, implying the increment in darkness. Meanwhile, the redness and yellowness intensity significantly increases as evidenced by the surge in a and b values as AgNPs concentration increased. The increase in darkness, yellowness, and redness of nanocomposite film leads to the reduction in whiteness index (WI) and the total color difference (ΔE). Similar results were illustrated by Shankar et al. on the combining of AgNPs into agar [36] and gelatin [46].

ATR-FTIR and XRD

The ATR-FTIR is used for the purpose of identifying the presence of functional groups and determining possible molecular interactions between components in the nanocomposite films. As illustrated in Fig. 4, the characteristic peak of the control PVA film at 3269 cm^{-1} is assigned to the O–H stretching vibrations; the peaks at 2938 cm^{-1} and 1245 cm^{-1} can be attributed to the C-H symmetric

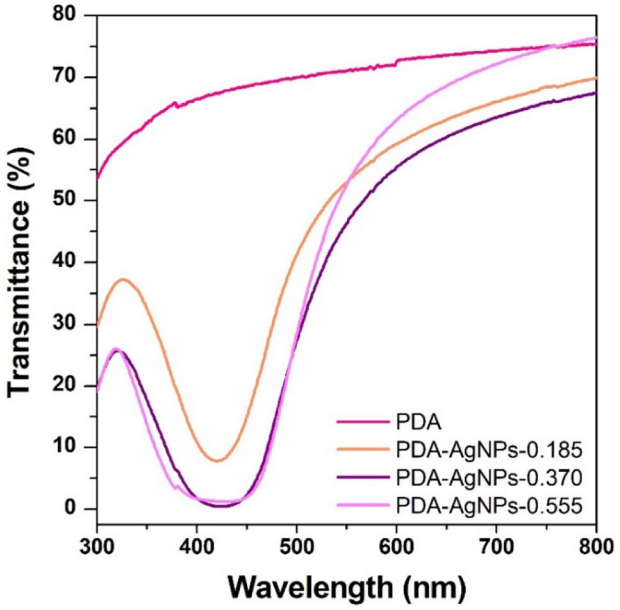

Fig. 2 Light transmittance of PDA film incorporated with AgNPs

stretching and CH-OH bending vibrations; the appearance of peaks at 1718 cm^{-1} and 1635 cm^{-1} are related to the C = O group stretching vibrations in amide I [47–49]. The peak at 1092 cm^{-1} is due to the C-O vibration in the crystalline region of PVA while that at 1035 cm^{-1} corresponds the C-O vibration in the amorphous region of PVA [50]. The co-incorporation of D-glucose, agar, and glycerol into PVA decreased the intensity of the peaks at 1245 cm^{-1} (CH-OH bending vibration), 1718 cm^{-1} and 1635 cm^{-1} (C = O stretching vibrations), and 1092 cm^{-1} (C-O stretching vibration). This possibly resulted from the formation of hydrogen bonds between PVA, D-glucose, agar, and glycerol.

Compared to PDA film, the ATR-FTIR spectra of nanocomposite film show no noticeable changes in characteristic peaks, indicating no new chemical bond formation. Notwithstanding, the revolution of peak at 1635 cm^{-1} in the nanocomposite films as AgNPs content increased from 0.370 mM to 0.555 mM, indicating the Van der Waals interaction between AgNPs molecules and polymer chains [45]. Similar results were reported by Roy et al. [45] and Sarwar et al. [6] as no chemical interactions are formed in carrageenan and PVA/nanocellulose film incorporated with AgNPs.

The XRD patterns of all the synthesized films are exhibited in Fig. 5. It is observed that the PVA film showed three diffraction peaks at 19.38°, 20.52°, and 40.32° linear with strong, medium, and weak intensity. This result indicates that PVA film is a semi-crystalline structure [51, 52]. The XRD pattern of PVA film combined with agar and D-glucose shows the increase in broadness and decrease in peak intensity in the range of 15°-25° as along with the disappearance at 40.32°. It is clear that the structure of PDA film tends to more amorphous state which is consistent with the above ATR-FTIR analysis. Similar result was found in the research of Pandit et al. on cross-linked PVA hydrogel [53]. After loading of 0.185 mM AgNPs into PDA film, the increase in broadness of diffraction peak at 22.52° is probably related to the heterogeneous distribution of AgNPs in polymer matrix. However, the peak intensity at 22.52° tends to weaken and fully disappear as the concentration of incorporated AgNPs increases from 0.370 mM to 0.555 mM. This means that the structure of resulting film become more amorphous. In brief, the structural order in film network is affected by AgNPs intercalation, which influence on the mechanical properties in the following study.

Mechanical properties

Thickness of films with and without of AgNPs is presented in Table 2. It can be seen that the thickness of all films is not significantly different. In order to avoid physical damage to the integrity of packed products during transport, storage, and use, the mechanical properties of the food packaging material are very crucial. The force resistance, mobility, and rigidness of all films are expressed by the values of tensile strength, elongation at break, and elastic

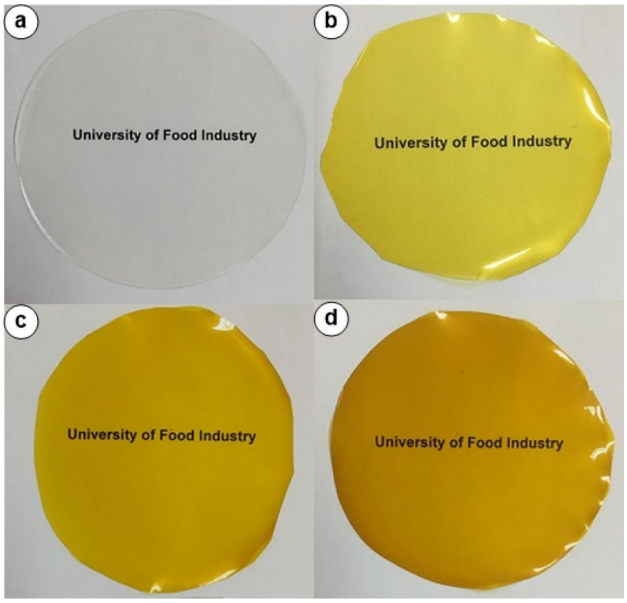

Fig. 3 Visual appearance of PDA (**a**), PDA-AgNPs-0.185 (**b**), PDA-AgNPs-0.370 (**c**), and PDA-AgNPs-0.555 (**d**) films

Table 1 Color, whiteness index and the total color difference of PDA films with and without AgNPs

Film samples	L	a	b	WI	E
PDA	$89.69^{a} \pm 0.62$	$-0.31^{d} \pm 0.03$	$5.20^{c} \pm 0.17$	88.45^{a}	4.19^{a}
PDA-AgNPs-0.185	$64.51^{b} \pm 0.42$	$7.51^{c} \pm 0.28$	$31.89^{a} \pm 0.21$	51.70^{b}	41.29^{b}
PDA-AgNPs-0.370	$60.27^{c} \pm 5.29$	$13.04^{b} \pm 1.11$	$33.54^{a} \pm 3.07$	46.40^{c}	46.71^{c}
PDA-AgNPs-0.555	$48.50^{d} \pm 1.87$	$17.67^{a} \pm 0.26$	$27.25^{b} \pm 1.05$	39.11^{d}	53.96^{d}

Values followed by the same letter at each column are not significantly different ($P < 0.05$). Data are accompanied by standard errors of the means ($n \geq 3$)

modulus. Tensile strength of PDA is 7.49 ± 0.45 MPa and this value is improved to 11.16 MPa, 12.09 MPa, and 12.08 MPa as the increment in AgNPs concentration from 0.185 mM to 0.555 mM into the polymer network. The nanoparticles were often reported to form physical interactions with polymer matrix thereby enhancing properties of the films. The increase in the tensile strengths of the resultant films was in agreement with the results obtained from other polymers incorporated with nanoparticles [54, 55]. In this study, tensile strengths of the three films loaded with AgNPs were not significantly different at different concentrations of AgNPs, much likely indicating that AgNPs only act as nanofillers via physical interactions, rather than having chemical interactions with PVA, D-glucose, agar, and glycerol. Similar finding was found in the kefiran films containing ZnO by Shahabi-Ghahfarrokhi et al. [55]. It is surprising that in the addition of 0.370–0.555 mM AgNPs results in considerable increase in the elongation at break values. This is consistent with XRD analysis when the structure of films tends to more amorphous after cooperating with AgNPs. In other words, AgNPs may act as a plasticizer to enhance the flexibility and mobility of the nanocomposite [56]. Similarly, Sarwar et al. [6] also reported the increment of elongation at break value of PVA/nanocellulose film after loading AgNPs. Also, the flexibility and mobility of starch film were improved by adding TiO_2 nanoparticles reported by Goudarzi et al. [57]. Besides, elastic modulus value decreases gradually as the increment of AgNPs content, which linear with the increase in flexibility and mobility in elongation at break. In summary, the addition of AgNPs into PDA film has dramatically improved the film's mechanical properties as great merit in food packaging area.

Contact angle and solubility

The contact angle is a parameter for determining the hydrophobic or hydrophilic properties of the film surface. The smaller the contact angle is, the higher the hydrophilicity is, and vice versa. The change in the film contact

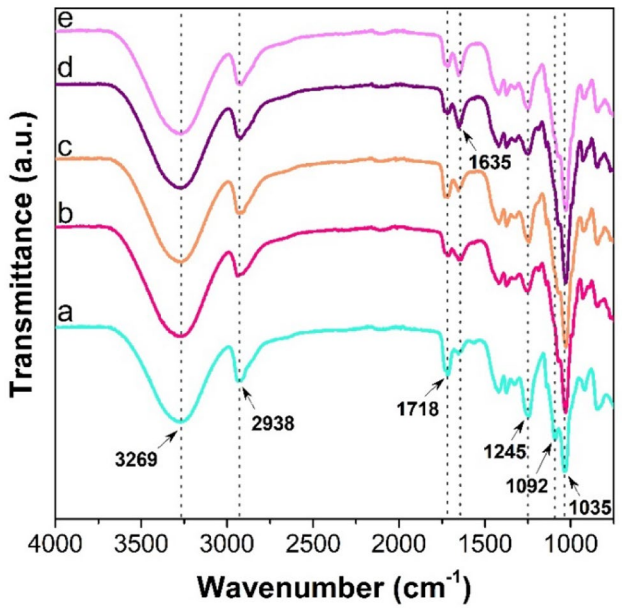

Fig. 4 ATR-FTIR spectra of PVA (**a**), PDA (**b**), PDA-AgNPs-0.185 (**c**), PDA-AgNPs-0.370 (**d**), and PDA-AgNPs-0.555 (**e**) films

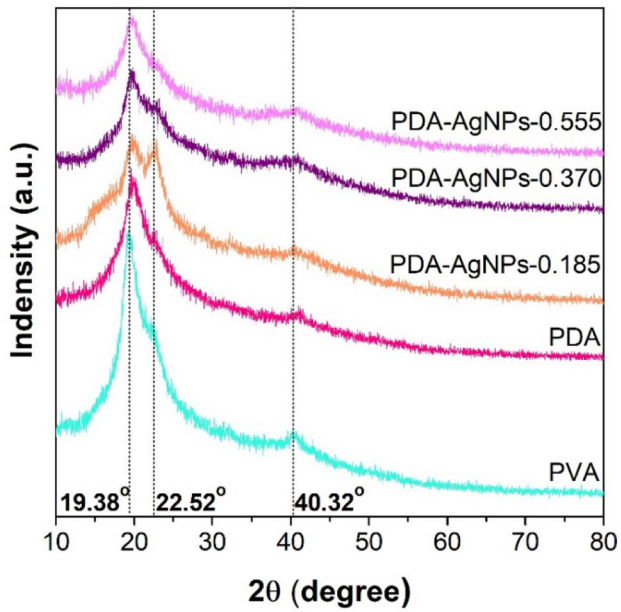

Fig. 5 XRD spectra of PDA, PDA-AgNPs-0.185, PDA-AgNPs-0.370, and PDA-AgNPs-0.555 films

Table 2 Thickness and mechanical behavior of PDA, PDA-AgNPs-185, PDA-AgNPs-370, and PDA-AgNPs-555 films

Film samples	Tensile strength (MPa)	Elongation at break (%)	Module young (MPa)	Thickness (mm)
PDA	$7.49^{b} \pm 0.45$	$179.59^{c} \pm 5.74$	$25.21^{b} \pm 0.57$	$0.105^{a} \pm 0.000$
PDA-AgNPs-0.185	$11.16^{a} \pm 0.83$	$170.29^{c} \pm 6.86$	$26.70^{b} \pm 1.11$	$0.102^{a} \pm 0.001$
PDA-AgNPs-0.370	$12.09^{a} \pm 0.28$	$237.12^{b} \pm 5.56$	$22.83^{a} \pm 0.69$	$0.100^{a} \pm 0.002$
PDA-AgNPs-0.555	$12.08^{a} \pm 0.37$	$300.24^{a} \pm 22.22$	$21.42^{a} \pm 0.90$	$0.097^{a} \pm 0.000$

Values followed by the same letter at each column are not significantly different ($P < 0.05$). Data are accompanied by standard errors of the means ($n \geq 3$)

angle as a function of time is displayed in Fig. 6. In general, the contact angle values rapidly decline in the first few seconds and gradually decrease in the further second for all films. After adding 0.185–0.555 mM AgNPs, the contact angle value of nanocomposite films considerably increases. This can be explained by the increment in the surface roughness of the films after combining with AgNPs [36, 58]. This result is consistent with SEM analysis as the surface roughness of PDA films surged upon the addition of AgNPs. Shankar and Rhim [36] and Huang et al. [58] were reported that the corporation of AgNPs into polydopamine/polysulfone and agar films, enhanced contact angle value due to surface roughness.

Visual observation showed that PVA film completely dissolved in water for about 3 min. Nonetheless, during the experimental process (24 h), PDA films with and without AgNPs were swollen in water. The solubilities of the PDA, PDA-AgNPs-0.185, PDA-AgNPs-0.370, and PDA-AgNPs-0.555 is recorded at $84.87 \pm 0.07\%$, $85.45 \pm 0.16\%$, $86.44 \pm 0.16\%$, and $86.70 \pm 0.09\%$, respectively. It can be concluded that the inclusion of AgNPs do not effect on the solubility of the nanocomposite films because no chemical interactions are formed as corroborated in the ATR-FTIR result.

Antimicrobial activities

Antimicrobial activity is one of the most crucial properties when the material is considered for food packaging applications. Figure 7 depicts antibacterial activities of nanocomposite films against *S. aureus*, *E. coli*, and *P. aeruginosa*. It can be seen that PDA film has no bactericidal effect against both Gram-negative (*E. coli* and *P. aeruginosa*) and Gram-positive (*S. aureus*) bacteria with the near-zero inhibitory zone (Supplementary Fig. S2). As expected, the loading AgNPs may enhance antimicrobial activity of resulting films. It can be observed that the antimicrobial activity increased with the increment of AgNPs content. Gram-negative bacteria were highly suppressed by PDA film loading AgNPs, meanwhile, the reduced susceptibility was found in against Gram-positive bacteria. It can be attributed to the difference in bacterial cell wall structure

Table 3 Weight loss, total soluble sugars, titratable acidity, and pH of Areca bananas during storage period

	Treatment	Storage time (days)				
		Day 1	Day 3	Day 4	Day 6	Day 7
Physiological loss in weight (%)	Uncoated	100	$92.26^{b} \pm 0.21$	$88.94^{b} \pm 0.47$	$80.28^{b} \pm 1.09$	$77.86^{b} \pm 1.25$
	Coated with PDA	100	$95.75^{a} \pm 0.16$	$93.80^{a} \pm 0.68$	$88.52^{a} \pm 0.61$	$86.89^{a} \pm 0.58$
	Coated with PDA-AgNPs-0.185	100	$95.48^{a} \pm 0.20$	$93.36^{a} \pm 0.21$	$87.76^{a} \pm 0.54$	$86.00^{a} \pm 0.60$
Total soluble sugars (%Brix)	Uncoated	$16.85^{b} \pm 0.21$	$26.05^{b} \pm 0.21$	$25.25^{b} \pm 1.63$	$27.35^{b} \pm 0.07$	$26.95^{b} \pm 1.63$
	Coated with PDA	$16.85^{b} \pm 0.21$	$23.65^{a} \pm 0.92$	$20.50^{a} \pm 0.14$	$24.50^{a} \pm 0.42$	$24.95^{a} \pm 0.35$
	Coated with PDA-AgNPs-0.185	$16.85^{a} \pm 0.21$	$22.40^{a} \pm 0.00$	$19.70^{a} \pm 0.57$	$23.00^{a} \pm 0.99$	$24.15^{a} \pm 0.07$
Titratable acidity (%)	Uncoated	4.02×10^{-2c}	3.18×10^{-2c}	2.51×10^{-2c}	2.68×10^{-2c}	2.35×10^{-2c}
	Coated with PDA	4.02×10^{-2a}	2.01×10^{-2a}	2.01×10^{-2b}	2.35×10^{-2b}	2.12×10^{-2b}
	Coated with PDA-AgNPs-0.185	4.02×10^{-2a}	2.01×10^{-2a}	1.68×10^{-2a}	2.01×10^{-2a}	2.01×10^{-2a}
pH	Uncoated	$5.00^{c} \pm 0.02$	$5.24^{c} \pm 0.04$	$5.38^{c} \pm 0.00$	$5.60^{c} \pm 0.07$	$5.92^{c} \pm 0.00$
	Coated with PDA	$5.00^{a} \pm 0.02$	$5.16^{a} \pm 0.03$	$5.22^{b} \pm 0.01$	$5.54^{b} \pm 0.01$	$5.82^{b} \pm 0.04$
	Coated with PDA-AgNPs-0.185	$5.00^{a} \pm 0.02$	$5.16^{a} \pm 0.05$	$5.19^{a} \pm 0.04$	$5.42^{a} \pm 0.05$	$5.62^{a} \pm 0.01$

Values followed by the same letter at each column are not significantly different ($P < 0.05$). Data are accompanied by standard errors of the means ($n \geq 3$)

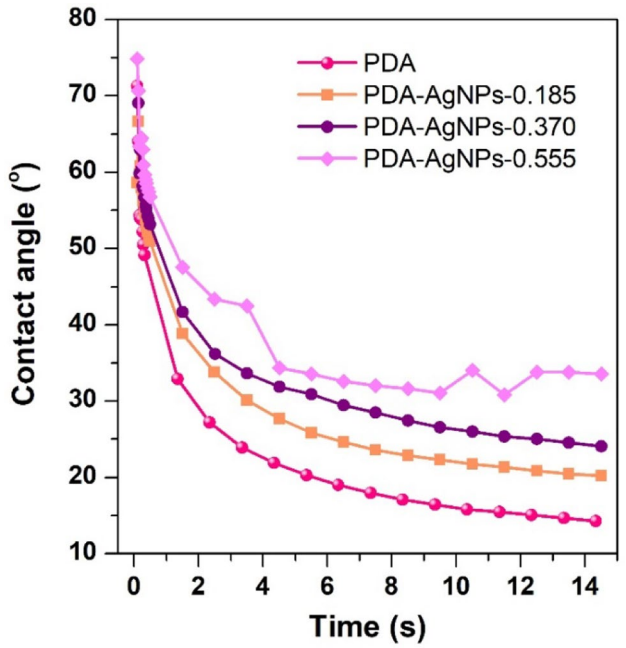

Fig. 6 Contact angle of PVA, PDA, PDA-AgNPs-0.185, PDA-AgNPs-0.370, and PDA-AgNPs-0.555 films

between Gram-negative and Gram-positive bacteria [35]. The multiplex cell wall structure of Gram-positive bacteria with thicker peptidoglycan (20–80 nm) hinders the penetration of AgNPs into bacterial cells [35, 59]. Conversely, a thinner layer (less than 10 nm) of Gram-negative bacteria is a favorable condition for AgNPs to penetrate conveniently [45, 59]. The PDA film loading AgNPs exhibited the strongest antibacterial activity against *P. aeruginosa*, confirmed by maximum inhibitory zone diameters at 13 mm, 17 mm, and 18 mm, respectively, for the PDA-AgNPs-0.185, PDA-AgNPs-0.370, and PDA-AgNPs-0.555. Briefly, the addition of AgNPs greatly improved the antimicrobial activity of the resultant film, indicating its potential application in food preservation.

Application for Areca banana preservation

The presence of oxygen in the environment surrounding the banana peel can facilitate oxidative polymerization of phenolics thus causing the growth of dark spots in the vicinity of the stomata on the banana peel surface [60, 61]. A coating, when being used, can cover rigidly all of the fruit surface, prevent direct contact between the fruit with the surrounding atmosphere and act as a barrier layer to gas exchange (O_2, CO_2, and C_2H_4) [62]. Herein, the PDA coating 0.185 mM AgNPs, the lowest AgNPs concentration, was selected to evaluate the fruit preservation effect. Bananas were dipped in PDA and PDA-AgNPs-0.185 solutions then stored at 25 ℃ and evaluated daily physicochemical properties including respiration rate, weight loss, total soluble solids, titratable acidity, and pH. The uncoated bananas were used as control sample.

Respiration rate

Banana is a climacteric fruit and is going to continue to ripen after harvest, leading to continued respiration and evaporation, which causes loss of shine and discoloration of peel, softening or shrinking, resulting in the decrease in flavor of the fruit [63]. The respiration process of fruits occurred as they used their nutrients to metabolize with oxygen and dihydrogen monoxide to break it down into end products such as carbon dioxide, dihydrogen monoxide and release energy [64]. In this study, the produced amount of CO_2 from uncoated bananas and bananas covered with PDA and PDA-AgNPs-0.185 in 7^{th} day storage is 405.38 ± 9.36 mg/kg.h, 362.00 ± 3.63 mg/kg.h and 370.21 ± 13.33 mg/kg.h, respectively. Coated bananas offer lower respiration rates because the coating may act as a selective barrier and thereby reducing internal-to-external gas exchange, leading to decrease respiration rate [41, 65]. On the other hand, the uncoated bananas released higher amount of CO_2 after 7 storage days, which is likely supported by the fact that bananas without coating respired stronger than coated bananas, accelerating the metabolism of glucose and fructose into CO_2 and water, and resulting in more produced CO_2 amount. Baez-Sanudo et al. [66] also reported a similar result with the highest CO_2 content generated from the uncoated bananas meanwhile the coated

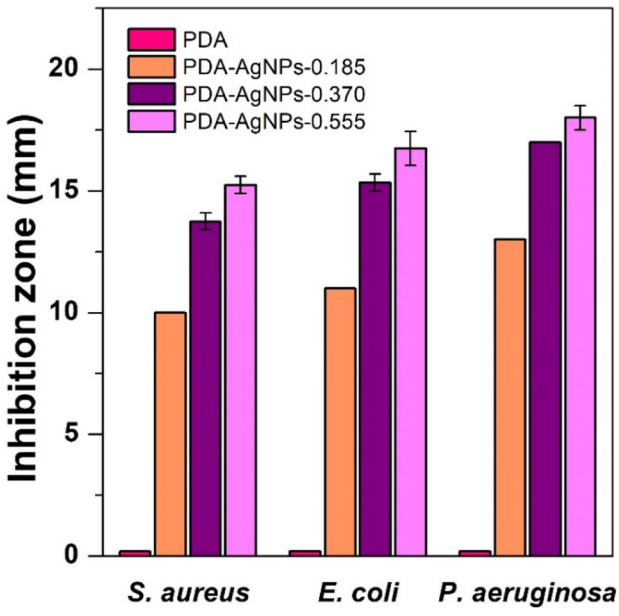

Fig. 7 Antibacterial activity of PDA films with and without loading AgNPs

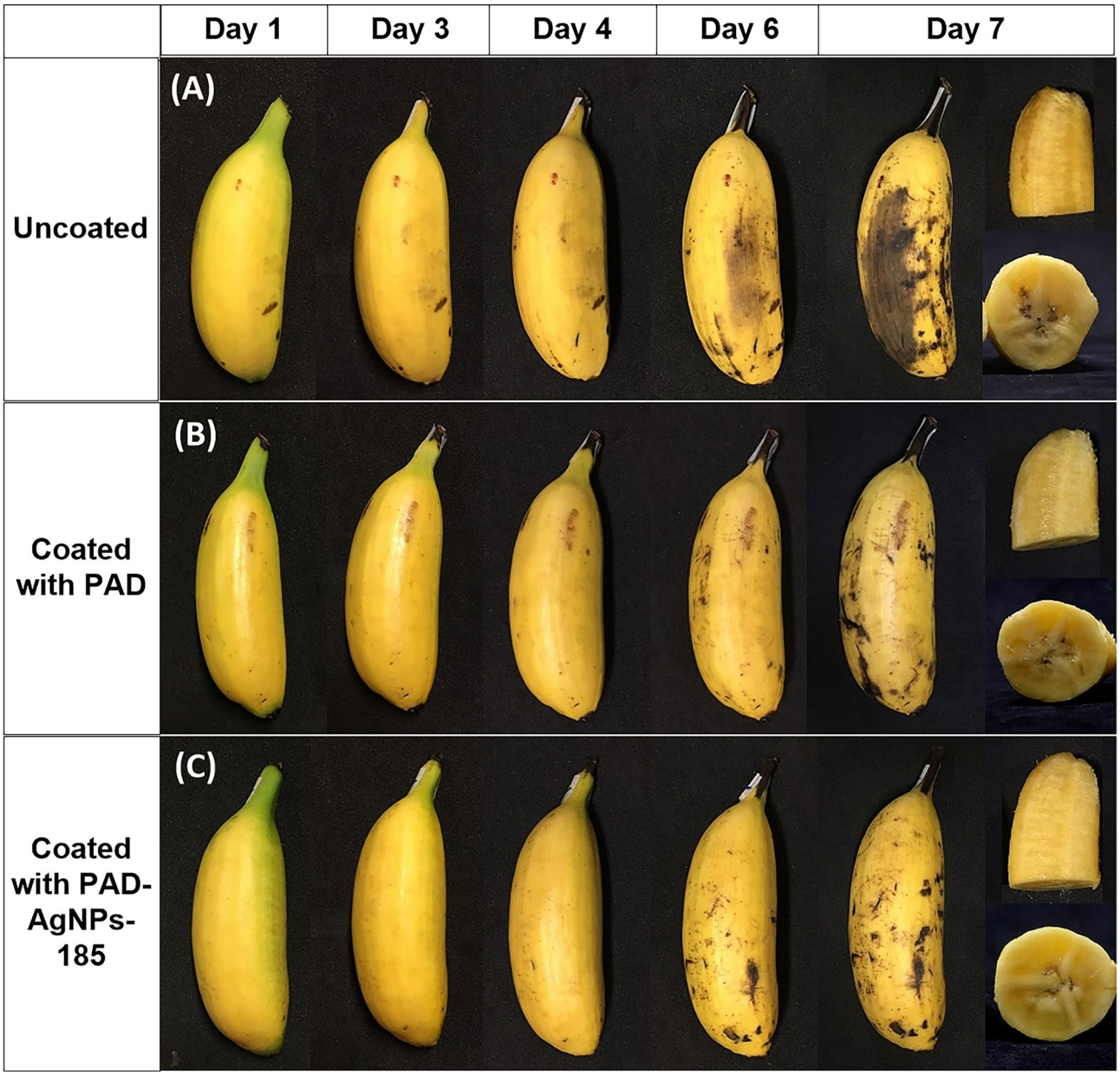

Fig. 8 The photos of uncoated banana (**a**), coated banana using PDA (**b**), and PDA-AgNPs-0.185 (**c**) solutions

bananas with 1-methyl cyclopropane and chitosan-based edible coating presented a lower respiration rate.

Physiological weight loss

The weight loss of bananas was closely related to respiration and evaporation rate during storage period, resulting in weight loss [67]. Table 3 presents the weight loss percentage of Areca banana after 7 days of storage. There is a significant difference in weight loss percentage owing to the treatments. The weight loss of uncoated fruits is recorded in the highest value ($22.14 \pm 1.25\%$) followed by the fruits coated with PDA-AgNPs-0.185 ($14.00 \pm 0.59\%$) and coated with PDA ($13.11 \pm 0.51\%$). It is clear that the coatings were more effective for preserving banana during storage period than uncoated fruit. The PDA and PDA-AgNPs-0.185 coatings may form a semi-permeable barrier against water vapor and gas loss, reducing the respiration rate and thus slowing down water loss, delaying the ripening process as well as the nutritional metabolism of the fruit. Similar result was reported by Toğrul and Arslan [68] that the surface coating help reduces moisture loss and gas exchange from the fruits. However, a slightly lower weight loss of the fruit coated with the PDA as compared to the one coated with PDA loading AgNPs is

observed. This result is consistent with the thickness of films and respiration rate values as the PDA coating is slightly thicker than the PDA coating incorporated with 0.185 mM AgNPs, resulting in slower water loss rate. Coating thickness playing a vital role in regulating the inner gas of the fruit that determines fruit quality during storage period [69].

The appearance of Areca banana

Respiration is also related to the change in peel color as well as softness and shrinkage. Figure 8 exhibits the change in the visual appearance of bananas after 7 days of storage. It can be observed that there is no considerable difference between the coated fruits; meanwhile, uncoated bananas showed the appearance of black spots, beginning on day 3^{th} and getting worse on day 6-7^{th}. After peeling the whole of banana peel, the pulp of uncoated fruits is crushed heavily, and the bottom of such bananas has dark-yellow color. In case of coated fruits, black spots appeared on 6^{th} day and spread by 7^{th} day. However, their decayed surface area is lower than that of the uncoated fruits. The main difference between coated fruits was found that the pulp of bananas with PDA-AgNPs-0.185 coating remains compact and does not appear any decayed zones. This indicates that adding AgNPs to the treatment would increase the protective efficiency of the banana during storage period.

Total soluble sugars concentration, titratable acidity, and pH

Total soluble sugars (TSS) consisting of carbohydrates, organic acids, and amino acids of fruit increases gradually during ripening owing to the hydrolysis of starch into sugars [70, 71]. Herein, the TSS of uncoated bananas increases rapidly from 16.85%Brix to 26.95%Brix after 7 days of storage period (Table 3). Meanwhile, the lower increment in TSS of PDA and PDA-AgNPs-0.185 covered bananas is found, suggesting that the coating could decrease the respiration rate and thereby decline the metabolism process in the fruit. Similarly, Hossain and Iqbal [72] reported that TSS was higher in the control banana sample than in the chitosan-coated sample.

In contrast to TSS, titratable acidity (TA) decreases over the whole storage period. Bananas without treatment present higher reduction in TA values as compared to coated bananas. This can be explained by the reduction in respiration rate of fruit and thus hindering TA consumption [73]. The pH value of PDA-AgNPs-0.185 shows the slowest increment as compared to bananas coated with PDA and uncoated fruits. The slight increase in pH value of fruits during storage period is linear with changes in TA. The TA and pH values of bananas coated with PDA-AgNPs-0.185 show the slowest acid metabolism, hence it is clearly that PDA loading AgNPs provides the best banana preservation performance. These results suggest that the introduction of AgNPs into PDA film may delay banana ripening, and demonstrate its feasibility in the preservation of agricultural products in the future.

Conclusion

Based on the obtained results, the PVA/D-glucose/agar film loading AgNPs was successfully developed by solvent casting technique. The combination of AgNPs into PVA modified with D-glucose and agar has improved the mechanical, hydrophobic, and antibacterial properties of the resulting film. The shelf life of bananas coated PDA-AgNPs and PDA is extended for 7 days at 25 ℃ as the appearance and nutrition are better than uncoated bananas. These results are demonstrated by physical weight loss, respiration rate, total soluble sugars content, pH, and titratable acidity measurement. Therefore, it can be concluded that PVA/D-glucose/agar film incorporated with AgNPs could be an effective approach for extending the shelf-life of tropical post harvested fruits.

Supplementary information The online version contains supplementary material available at https://doi.org/10.1007/s10965-021-02761-1.

Acknowledgements This research is funded by Nguyen Tat Thanh University, Ho Chi Minh city, Vietnam (2020.01.148).

Declarations

Conflict of interest The authors declare that they have no known competing financial interests or personal relationships that could have appeared to influence the work reported in this paper.

References

1. Garlotta D (2001) Literature Review of Poly(Lactic Acid). J Polym Environ 9:63–84. https://doi.org/10.1023/A:1020200822435
2. Hari N, Francis S, Rajendran Nair AG, Nair AJ (2018) Synthesis, characterization and biological evaluation of chitosan film incorporated with β-Carotene loaded starch nanocrystals. Food Packag Shelf Life 16:69–76. https://doi.org/10.1016/j.fpsl.2018.02.003
3. Kaya M, Khadem S, Cakmak YS et al (2018) Antioxidative and antimicrobial edible chitosan films blended with stem, leaf and seed extracts of Pistacia terebinthus for active food packaging. RSC Adv 8:3941–3950. https://doi.org/10.1039/c7ra12070b
4. Mahdavi V, Hosseini SE, Sharifan A (2018) Effect of edible chitosan film enriched with anise (Pimpinella anisum L.) essential oil on shelf life and quality of the chicken burger. Food Sci Nutr 6:269–279. https://doi.org/10.1002/fsn3.544
5. Lizardi-Mendoza J, Argüelles Monal WM, Goycoolea Valencia FM (2016) Chemical Characteristics and Functional Properties of Chitosan. In: Chitosan in the Preservation of Agricultural Commodities. Elsevier 3–31. https://doi.org/10.1016/B978-0-12-802735-6.00001-X

6. Sarwar MS, Niazi MBK, Jahan Z et al (2018) Preparation and characterization of PVA/nanocellulose/Ag nanocomposite films for antimicrobial food packaging. Carbohydr Polym 184:453–464. https://doi.org/10.1016/j.carbpol.2017.12.068
7. Wang W, Yu Z, Alsammarraie FK et al (2020) Properties and antimicrobial activity of polyvinyl alcohol-modified bacterial nanocellulose packaging films incorporated with silver nanoparticles. Food Hydrocoll 100:105411. https://doi.org/10.1016/j.foodhyd.2019.105411
8. Mustafa P, Niazi MBK, Jahan Z et al (2020) PVA/starch/propolis/anthocyanins rosemary extract composite films as active and intelligent food packaging materials. J Food Saf 40:1–11. https://doi.org/10.1111/jfs.12725
9. Zhai X, Shi J, Zou X et al (2017) Novel colorimetric films based on starch/polyvinyl alcohol incorporated with roselle anthocyanins for fish freshness monitoring. Food Hydrocoll 69:308–317. https://doi.org/10.1016/j.foodhyd.2017.02.014
10. Cano A, Cháfer M, Chiralt A, González-Martínez C (2016) Development and characterization of active films based on starch-PVA, containing silver nanoparticles. Food Packag Shelf Life 10:16–24. https://doi.org/10.1016/j.fpsl.2016.07.002
11. Kanmani P, Rhim JW (2014) Physicochemical properties of gelatin/silver nanoparticle antimicrobial composite films. Food Chem 148:162–169. https://doi.org/10.1016/j.foodchem.2013.10.047
12. Wu J, Sun X, Guo X et al (2017) Physicochemical properties, antimicrobial activity and oil release of fish gelatin films incorporated with cinnamon essential oil. Aquac Fish 2:185–192. https://doi.org/10.1016/j.aaf.2017.06.004
13. Abdullah ZW, Dong Y, Davies IJ, Barbhuiya S (2017) PVA, PVA Blends, and Their Nanocomposites for Biodegradable Packaging Application. Polym Plast Technol Eng 56:1307–1344. https://doi.org/10.1080/03602559.2016.1275684
14. Mathews S, Hans M, Mücklich F, Solioz M (2013) Contact killing of bacteria on copper is suppressed if bacterial-metal contact is prevented and is induced on iron by copper ions. Appl Environ Microbiol 79:2605–2611. https://doi.org/10.1128/AEM.03608-12
15. Yang W, Owczarek JS, Fortunati E et al (2016) Antioxidant and antibacterial lignin nanoparticles in polyvinyl alcohol/chitosan films for active packaging. Ind Crops Prod 94:800–811. https://doi.org/10.1016/j.indcrop.2016.09.061
16. Miranda TMR, Gonçalves AR, Amorim MTP (2001) Ultraviolet-induced crosslinking of poly(vinyl alcohol) evaluated by principal component analysis of FTIR spectra. Polym Int 50:1068–1072. https://doi.org/10.1002/pi.745
17. El-Mohdy HLA (2007) Synthesis of starch-based plastic films by electron beam irradiation. J Appl Polym Sci 104:504–513. https://doi.org/10.1002/app.25524
18. Gao H, Yang H (2017) Characteristics of poly(vinyl alcohol) films crosslinked by cinnamaldehyde with improved transparency and water resistance. J Appl Polym Sci 134:1–8. https://doi.org/10.1002/app.45324
19. Tripathi S, Mehrotra GK, Dutta PK (2009) Physicochemical and bioactivity of cross-linked chitosan-PVA film for food packaging applications. Int J Biol Macromol 45:372–376. https://doi.org/10.1016/j.ijbiomac.2009.07.006
20. Figueiredo KCS, Alves TLM, Borges CP (2009) Poly(vinyl alcohol) films crosslinked by glutaraldehyde under mild conditions. J Appl Polym Sci 111:3074–3080. https://doi.org/10.1002/app.29263
21. Debeaufort F, Voilley A (2009) Edible Films and Coatings for Food Applications. Springer, New York, New York, NY. https://doi.org/10.1007/978-0-387-92824-1
22. Madera-Santana TJ, Freile-Pelegrín Y, Azamar-Barrios JA (2014) Physicochemical and morphological properties of plasticized poly(vinyl alcohol)-agar biodegradable films. Int J Biol Macromol 69:176–184. https://doi.org/10.1016/j.ijbiomac.2014.05.044
23. Castro N, Durrieu V, Raynaud C, Rouilly A (2016) Influence of DE-value on the physicochemical properties of maltodextrin for melt extrusion processes. Carbohydr Polym 144:464–473. https://doi.org/10.1016/j.carbpol.2016.03.004
24. Nguyen TT, Phung TK, Bui X et al (2021) Removal of cationic dye using polyvinyl alcohol membrane functionalized by D-glucose and agar. J Water Process Eng 40:101982. https://doi.org/10.1016/j.jwpe.2021.101982
25. Chen C, Xu Z, Ma Y et al (2018) Properties, vapour-phase antimicrobial and antioxidant activities of active poly(vinyl alcohol) packaging films incorporated with clove oil. Food Control 88:105–112. https://doi.org/10.1016/j.foodcont.2017.12.039
26. Narasagoudr SS, Hegde VG, Vanjeri VN et al (2020) Ethyl vanillin incorporated chitosan/poly(vinyl alcohol) active films for food packaging applications. Carbohydr Polym 236:116049. https://doi.org/10.1016/j.carbpol.2020.116049
27. Liu Y, Wang S, Lan W (2018) Fabrication of antibacterial chitosan-PVA blended film using electrospray technique for food packaging applications. Int J Biol Macromol 107:848–854. https://doi.org/10.1016/j.ijbiomac.2017.09.044
28. Musetti A, Paderni K, Fabbri P et al (2014) Poly(vinyl alcohol)-Based Film Potentially Suitable for Antimicrobial Packaging Applications. J Food Sci 79:E577–E582. https://doi.org/10.1111/1750-3841.12375
29. Nur Amila Najwa IS, Mat Yusoff M, Nur Hanani ZA (2020) Potential of Silver-Kaolin in Gelatin Composite Films as Active Food Packaging Materials. Food Packag Shelf Life 26:100564. https://doi.org/10.1016/j.fpsl.2020.100564
30. Kowsalya E, MosaChristas K, Balashanmugam P et al (2019) Biocompatible silver nanoparticles/poly(vinyl alcohol) electrospun nanofibers for potential antimicrobial food packaging applications. Food Packag Shelf Life 21:100379. https://doi.org/10.1016/j.fpsl.2019.100379
31. Carbone M, Donia DT, Sabbatella G, Antiochia R (2016) Silver nanoparticles in polymeric matrices for fresh food packaging. J King Saud Univ - Sci 28:273–279. https://doi.org/10.1016/j.jksus.2016.05.004
32. Lansdown ABG (2002) Silver I: its antibacterial properties and mechanism of action. J Wound Care 11:125–130. https://doi.org/10.12968/jowc.2002.11.4.26389
33. Pencheva D, Bryaskova R, Kantardjiev T (2012) Polyvinyl alcohol/silver nanoparticles (PVA/AgNps) as a model for testing the biological activity of hybrid materials with included silver nanoparticles. Mater Sci Eng C 32:2048–2051. https://doi.org/10.1016/j.msec.2012.05.016
34. Batool S, Hussain Z, Niazi MBK et al (2019) Biogenic synthesis of silver nanoparticles and evaluation of physical and antimicrobial properties of Ag/PVA/starch nanocomposites hydrogel membranes for wound dressing application. J Drug Deliv Sci Technol 52:403–414. https://doi.org/10.1016/j.jddst.2019.05.016
35. Shankar S, Rhim JW (2017) Preparation and characterization of agar/lignin/silver nanoparticles composite films with ultraviolet light barrier and antibacterial properties. Food Hydrocoll 71:76–84. https://doi.org/10.1016/j.foodhyd.2017.05.002
36. Shankar S, Rhim JW (2015) Amino acid mediated synthesis of silver nanoparticles and preparation of antimicrobial agar/silver nanoparticles composite films. Carbohydr Polym 130:353–363. https://doi.org/10.1016/j.carbpol.2015.05.018
37. Chen C-H, Lin Y-C, Mao C-F, Liao W-T (2019) Green synthesis, size control, and antibacterial activity of silver nanoparticles on chitosan films. Res Chem Intermed 45:4463–4472. https://doi.org/10.1007/s11164-019-03842-z
38. Ahmad M, Benjakul S, Prodpran T, Agustini TW (2012) Physico-mechanical and antimicrobial properties of gelatin film from the skin of unicorn leatherjacket incorporated with essential oils. Food Hydrocoll 28:189–199. https://doi.org/10.1016/j.foodhyd.2011.12.003

39. Mittal A, Garg S, Kohli D et al (2016) Effect of cross linking of PVA/starch and reinforcement of modified barley husk on the properties of composite films. Carbohydr Polym 151:926–938. https://doi.org/10.1016/j.carbpol.2016.06.037
40. Tepe B, Daferera D, Sokmen A et al (2005) Antimicrobial and antioxidant activities of the essential oil and various extracts of Salvia tomentosa Miller (Lamiaceae). Food Chem 90:333–340. https://doi.org/10.1016/j.foodchem.2003.09.013
41. Jongsri P, Wangsomboondee T, Rojsitthisak P, Seraypheap K (2016) Effect of molecular weights of chitosan coating on postharvest quality and physicochemical characteristics of mango fruit. LWT 73:28–36. https://doi.org/10.1016/j.lwt.2016.05.038
42. Kumar P, Selvi SS, Govindaraju M (2012) Seaweed-mediated biosynthesis of silver nanoparticles using Gracilaria corticata for its antifungal activity against Candida spp. Appl Nanosci 3:1–7. https://doi.org/10.1007/s13204-012-0151-3
43. Ananth AN, Umapathy S, Sophia J et al (2011) On the optical and thermal properties of in situ/ex situ reduced Ag NP's/PVA composites and its role as a simple SPR-based protein sensor. Appl Nanosci 1:87–96. https://doi.org/10.1007/s13204-011-0010-7
44. Elshaarawy RFM, Seif GA, El-Naggar ME et al (2019) In-situ and ex-situ synthesis of poly-(imidazolium vanillyl)-grafted chitosan/silver nanobiocomposites for safe antibacterial finishing of cotton fabrics. Eur Polym J 116:210–221. https://doi.org/10.1016/j.eurpolymj.2019.04.013
45. Roy S, Shankar S, Rhim JW (2019) Melanin-mediated synthesis of silver nanoparticle and its use for the preparation of carrageenan-based antibacterial films. Food Hydrocoll 88:237–246. https://doi.org/10.1016/j.foodhyd.2018.10.013
46. Shankar S, Jaiswal L, Selvakannan PR et al (2016) Gelatin-based dissolvable antibacterial films reinforced with metallic nanoparticles. RSC Adv 6:67340–67352. https://doi.org/10.1039/c6ra10620j
47. Nugraheni AD, Purnawati D et al (2016) Study of thermal degradation of PVA/Chitosan/Gelatin electrospun nanofibers. 150017. https://doi.org/10.1063/1.4958590
48. Nouri L, Mohammadi Nafchi A (2014) Antibacterial, mechanical, and barrier properties of sago starch film incorporated with betel leaves extract. Int J Biol Macromol 66:254–259. https://doi.org/10.1016/j.ijbiomac.2014.02.044
49. Hu D, Wang L (2016) Fabrication of antibacterial blend film from poly (vinyl alcohol) and quaternized chitosan for packaging. Mater Res Bull 78:46–52. https://doi.org/10.1016/j.materresbull.2016.02.025
50. Mansur HS, Sadahira CM, Souza AN, Mansur AAP (2008) FTIR spectroscopy characterization of poly (vinyl alcohol) hydrogel with different hydrolysis degree and chemically crosslinked with glutaraldehyde. Mater Sci Eng C 28:539–548. https://doi.org/10.1016/j.msec.2007.10.088
51. Costa-Júnior ES, Barbosa-Stancioli EF, Mansur AAP et al (2009) Preparation and characterization of chitosan/poly(vinyl alcohol) chemically crosslinked blends for biomedical applications. Carbohydr Polym 76:472–481. https://doi.org/10.1016/j.carbpol.2008.11.015
52. Gan Y, Bai S, Hu S et al (2016) Reaction mechanism of thermally-induced electric conduction of poly(vinyl alcohol)-silver nitrate hybrid films. RSC Adv 6:56728–56737. https://doi.org/10.1039/c6ra08994a
53. Pandit AH, Mazumdar N, Imtiyaz K et al (2019) Periodate-Modified Gum Arabic Cross-linked PVA Hydrogels: A Promising Approach toward Photoprotection and Sustained Delivery of Folic Acid. ACS Omega 4:16026–16036. https://doi.org/10.1021/acsomega.9b02137
54. Dehghani S, Peighambardoust SH, Peighambardoust SJ et al (2019) Improved mechanical and antibacterial properties of active LDPE films prepared with combination of Ag, ZnO and CuO nanoparticles. Food Packag Shelf Life 22:100391. https://doi.org/10.1016/j.fpsl.2019.100391
55. Shahabi-Ghahfarrokhi I, Khodaiyan F, Mousavi M, Yousefi H (2015) Preparation of UV-protective kefiran/nano-ZnO nanocomposites: Physical and mechanical properties. Int J Biol Macromol 72:41–46. https://doi.org/10.1016/j.ijbiomac.2014.07.047
56. Nguyen N-T, Liu J-H (2014) A green method for in situ synthesis of poly(vinyl alcohol)/chitosan hydrogel thin films with entrapped silver nanoparticles. J Taiwan Inst Chem Eng 45:2827–2833. https://doi.org/10.1016/j.jtice.2014.06.017
57. Goudarzi V, Shahabi-Ghahfarrokhi I, Babaei-Ghazvini A (2017) Preparation of ecofriendly UV-protective food packaging material by starch/TiO2 bio-nanocomposite: Characterization. Int J Biol Macromol 95:306–313. https://doi.org/10.1016/j.ijbiomac.2016.11.065
58. Huang L, Zhao S, Wang Z et al (2016) In situ immobilization of silver nanoparticles for improving permeability, antifouling and anti-bacterial properties of ultrafiltration membrane. J Memb Sci 499:269–281. https://doi.org/10.1016/j.memsci.2015.10.055
59. Salari M, Sowti Khiabani M, Rezaei Mokarram R et al (2018) Development and evaluation of chitosan based active nanocomposite films containing bacterial cellulose nanocrystals and silver nanoparticles. Food Hydrocoll 84:414–423. https://doi.org/10.1016/j.foodhyd.2018.05.037
60. Pongprasert N, Srilaong V, Sunpapao A (2021) Postharvest senescent dark spot development mechanism of Musa acuminata ("Khai" banana) peel associated with chlorophyll degradation and stomata cell death. J Food Biochem 45:e13745. https://doi.org/10.1111/jfbc.13745
61. Moser S, Müller T, Holzinger A et al (2009) Fluorescent chlorophyll catabolites in bananas light up blue halos of cell death. Proc Natl Acad Sci 106:15538–15543. https://doi.org/10.1073/pnas.0908060106
62. Kumari M, Mahajan H, Joshi R, Gupta M (2017) Development and structural characterization of edible films for improving fruit quality. Food Packag Shelf Life 12:42–50. https://doi.org/10.1016/j.fpsl.2017.02.003
63. Mattoo AK (2019) Postharvest Physiology and Biochemistry of Fruits and Vegetables. Elsevier, México. https://doi.org/10.1016/C2016-0-04653-3
64. Saltveit ME (2000) Measuring respiration Univiesity Calif Davis 95616:1–5
65. Meindrawan B, Suyatma NE, Wardana AA, Pamela VY (2018) Nanocomposite coating based on carrageenan and ZnO nanoparticles to maintain the storage quality of mango. Food Packag Shelf Life 18:140–146. https://doi.org/10.1016/j.fpsl.2018.10.006
66. Baez-Sañudo M, Siller-Cepeda J, Muy-Rangel D, Heredia JB (2009) Extending the shelf-life of bananas with 1-methylcyclopropene and a chitosan-based edible coating. J Sci Food Agric 89:2343–2349. https://doi.org/10.1002/jsfa.3715
67. Hailu M, Seyoum Workneh T, Belew D (2014) Effect of packaging materials on shelf life and quality of banana cultivars (Musa spp.). J Food Sci Technol 51:2947–2963. https://doi.org/10.1007/s13197-012-0826-5
68. Toğrul H, Arslan N (2004) Extending shelf-life of peach and pear by using CMC from sugar beet pulp cellulose as a hydrophilic polymer in emulsions. Food Hydrocoll 18:215–226. https://doi.org/10.1016/S0268-005X(03)00066-3
69. Cisneros-Zevallos L, Krochta JM (2005) Internal modified atmospheres of coated fresh fruits and vegetables: Understanding relative humidity effects*. In: Innovations in Food Packaging. Elsevier 173–184. https://doi.org/10.1016/B978-012311632-1/50043-7
70. Zheng K, Xiao S, Li W et al (2019) Chitosan-acorn starch-eugenol edible film: Physico-chemical, barrier, antimicrobial, antioxidant and structural properties. Int J Biol Macromol 135:344–352. https://doi.org/10.1016/j.ijbiomac.2019.05.151

71. Cano MP, de Ancos B, Matallana MC et al (1997) Differences among Spanish and Latin-American banana cultivars: morphological, chemical and sensory characteristics. Food Chem 59:411–419. https://doi.org/10.1016/S0308-8146(96)00285-3
72. Hossain MS, Iqbal A (2016) Effect of shrimp chitosan coating on postharvest quality of banana (Musa sapientum L.) fruits. Int Food Res J 23:277–283
73. Xu D, Qin H, Ren D (2018) Prolonged preservation of tangerine fruits using chitosan/montmorillonite composite coating. Postharvest Biol Technol 143:50–57. https://doi.org/10.1016/j.postharvbio.2018.04.013